

Charge transfer in nanocrystalline-Au/ZnO nanorods investigated by x-ray spectroscopy and scanning photoelectron microscopy

J. W. Chiou, S. C. Ray, H. M. Tsai, C. W. Pao, F. Z. Chien, and W. F. Pong^{a)}
Department of Physics, Tamkang University, Tamsui 251, Taiwan

M.-H. Tsai
Department of Physics, National Sun Yat-Sen University, Kaohsiung 804, Taiwan

J. J. Wu and C. H. Tseng
Department of Chemical Engineering, National Cheng Kung University, Tainan 701, Taiwan

C.-H. Chen and J. F. Lee
National Synchrotron Radiation Research Center, Hsinchu 300, Taiwan

J.-H. Guo
Advanced Light Source, Lawrence Berkeley National Laboratory, Berkeley, California 94720

(Received 22 March 2007; accepted 17 April 2007; published online 9 May 2007)

O *K*- and Zn and Au *L*₃-edge x-ray absorption near-edge structure (XANES), x-ray emission spectroscopy (XES), and scanning photoelectron microscopy (SPEM) are performed to investigate the electronic structure of ZnO nanorods with nanocrystalline (*nc*)-Au particles grown on the surfaces. The XANES spectra of *nc*-Au/ZnO nanorods reveal the decrease of the number of both O 2*p* and Zn 4*s*/3*d* unoccupied states with the increase of the *nc*-Au particle size. The number of Au 6*s*/5*d* unoccupied states increases when the size of *nc*-Au particle decreases, indicating that the deposition of *nc*-Au particles on the surface of ZnO nanorods promotes charge transfer from the ZnO nanorods to *nc*-Au particles. Excitation energy dependent XES and SPEM spectra show that the number of electrons in the valence band of O 2*p*-Zn 4*sp* hybridized states decreases as the *nc*-Au particle size increases, revealing that more electrons are excited from the valence band to the conduction band of ZnO nanorods and the storage of electrons in *nc*-Au particles. © 2007 American Institute of Physics. [DOI: 10.1063/1.2738369]

Among semiconductors, ZnO and TiO₂ have been recognized as preferable photocatalysis materials because of their high photosensitivity, nontoxicity, large band gap, and chemical stability.¹ The photocatalytic activities were found to be enhanced when noble metals such as Au, Ag, Cu, and Pt nanoparticles were deposited on these semiconductors because the metal nanoparticles store electrons within them.^{2,3} Wood *et al.* observed that the Fermi level (*E*_{*f*}) shifted toward conduction-band energy level in the metal-ZnO quantum dots, which increased the efficiency of photocatalytic reactions.³ In principle, the noble metal acts as a sink, improving interfacial charge transfer associated with the photo-induced electron-hole separation in the photocatalytic process. The photocatalytic properties of nanocrystalline (*nc*)-Au/ZnO nanorods for various UV irradiation periods have been studied by Wu and Tseng.⁴ This work focuses on how the conduction and valence bands of ZnO nanorods are changed and the correlation between charge transfer and the size of the *nc*-Au particles grown on the surface of ZnO nanorods using x-ray absorption near-edge structure (XANES), x-ray emission spectroscopy (XES), and scanning photoelectron microscopy (SPEM). The present study will further provide specific information of electronic states on the O and Zn sites and the role played by *nc*-Au particles on the charge separation in *nc*-Au/ZnO nanorods, which has not been well understood.

Zn, Au *L*₃-edge XANES, and SPEM were performed at the National Synchrotron Radiation Research Center in Hsin-

chu, Taiwan. XES and corresponding XANES measurements of the O *K* edge were carried out at beamline-7.0.1 at the Advanced Light Source, Lawrence Berkeley National Laboratory. The *nc*-Au particles grown on the vertically aligned ZnO nanorods were photosynthesized in various concentrations of HAuCl₄/ethanol and irradiated with 365 nm UV. Three samples denoted by S-3-10, S-4-10, and S-5-30 correspond to the ZnO nanorods that were irradiated under UV in 1 × 10⁻³, 1 × 10⁻⁴, and 1 × 10⁻⁵ M HAuCl₄/ethanol solutions for 10, 10, and 30 min, respectively. The sizes of *nc*-Au particles (*d*_{Au}) are ~30, 15, and 5 nm, respectively, for samples S-3-10, S-4-10, and S-5-30. Pure ZnO nanorods deposited on the Si substrate were also used for comparison.

Figure 1 presents the x-ray diffraction (XRD) spectra of *nc*-Au/ZnO nanorods with various sizes of *nc*-Au particles and pure ZnO nanorods. The XRD spectrum of sample S-3-10 has a strong *nc*-Au characteristic feature at $\theta \approx 38^\circ$. In contrast, this feature is very weak in the spectrum of sample S-4-10 and is absent in that of sample S-5-30. This is because nanocrystalline Au particles grown in very dilute HAuCl₄/ethanol solutions were expected to be small and dilute and were less likely to be detected by XRD. The secondary electron image (SEI) and corresponding backscattering electron images (BEI) of sample S-4-10 shown in the insets (a) and (b) of Fig. 1, clearly reveal that *nc*-Au particles are distributed all over the surfaces of ZnO nanorods. The inset (c) of Fig. 1 shows the high-resolution transmission electron microscopy (HRTEM) image of sample S-5-30, which contains images of *nc*-Au particles on the surface of ZnO nanorods. Details of sample preparations and their photocatalytic behaviors can be found elsewhere.⁴

^{a)} Author to whom correspondence should be addressed; electronic mail: wfpong@mail.tku.edu.tw

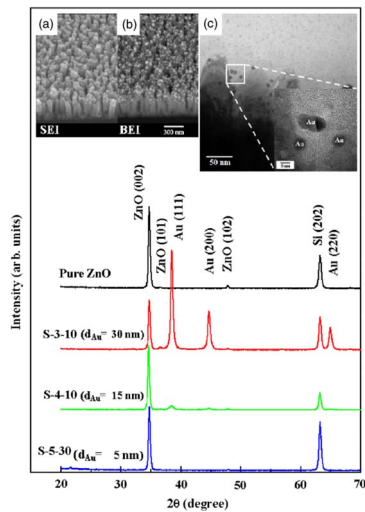


FIG. 1. (Color online) XRD spectra of the *nc*-Au/ZnO nanorods and pure ZnO nanorods. The upper left insets are (a) SEI and (b) BEI of sample S-4-10 and the upper right inset (c) is the HRTEM image of sample S-5-30 with the corresponding *nc*-Au particles shown.

Figure 2 displays normalized O *K*-edge XANES spectra of the various *nc*-Au/ZnO nanorods and pure ZnO nanorods. Features in the energy range of 530–545 eV were attributed to electron transitions from O 1s to 2p_σ (along the bilayer) and O 2p_π (along the c axis) states.^{5–8} The intensities of these features for *nc*-Au/ZnO nanorods are reduced relative to those of pure ZnO nanorods and the amount of reduction increases with the size of the *nc*-Au particles, which indicates that the number of O 2p unoccupied states of the *nc*-Au/ZnO nanorods is less than that of pure ZnO nanorods and decreases with the increase of the size of the *nc*-Au particles. The lower inset in Fig. 2 displays normalized Zn *L*₃-edge XANES spectra of *nc*-Au/ZnO nanorods and pure ZnO nanorods. The features between 1012 and 1027 eV are associated with the transition of Zn 2p electrons to 4s/3d states.^{5,6} The intensities of these *nc*-Au/ZnO nanorod features also decrease like those in the O *K*-edge XANES spectra as the *nc*-Au particle size increases and are smaller than those of pure ZnO nanorods. In contrast, as presented in the upper inset of Fig. 2, the intensities of the various features in

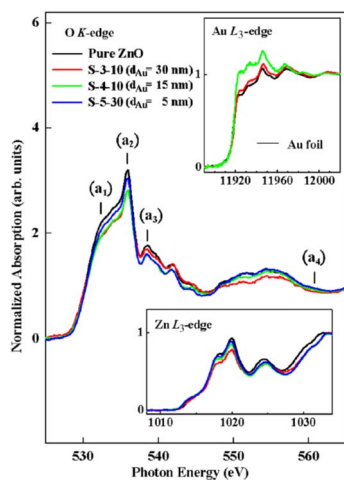


FIG. 2. (Color online) O *K*-edge XANES spectra of *nc*-Au/ZnO nanorods and pure ZnO nanorods. The upper inset displays Au *L*₃-edge XANES spectra of *nc*-Au/ZnO nanorods and the lower inset displays Zn *L*₃-edge XANES spectra of *nc*-Au/ZnO nanorods and pure ZnO nanorods.

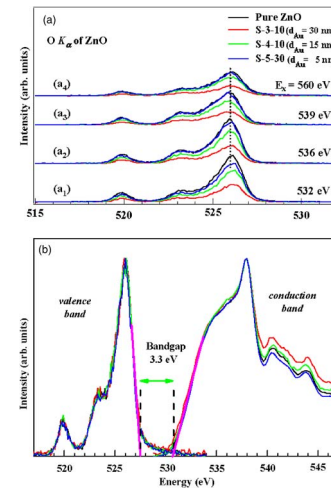


FIG. 3. (Color online) (a) Comparison of the XES spectra of *nc*-Au/ZnO nanorods with that of pure ZnO nanorods at selected excitation energies E_x ; (b) XES and corresponding XANES spectra of O 2p states of *nc*-Au/ZnO nanorods and pure ZnO nanorods.

the Au *L*₃-edge XANES spectra of *nc*-Au/ZnO nanorods are larger than those of the reference Au foil and the intensities increase as the particle size of *nc*-Au decreases. In pure Au, according to the dipole-transition selection rules, these features correspond mainly to the Au 2p_{3/2} to 6s/5d transitions.^{9,10} Although Au 5d orbitals are full for a free Au atom, Au 5d states can be observed at the edge because of *s-p-d* rehybridization.¹⁰ Note that the Au *L*₃-edge XANES spectrum could not be obtained for sample S-5-30 similar to the XRD spectrum because of small coverage. The results of the Au *L*₃-edge XANES for *nc*-Au/ZnO nanorods can be interpreted as an increase of electron transfer for larger *nc*-Au particles. The reduction of the number of Au 6s/5d unoccupied states indicates that the larger *nc*-Au particles gain more electrons from the ZnO nanorods. Hence, the charge separation capacity of the *nc*-Au particles depends strongly on their sizes, leading to the XANES results shown in Fig. 2.

Figure 3(a) displays the O *K*α emission spectra of *nc*-Au/ZnO nanorods and pure ZnO nanorods obtained at various excitation energies E_x , which are denoted by a_1 , a_2 , a_3 , and a_4 in Fig. 2 of the O *K*-edge XANES spectra, to study the predominant contribution of specific admixture of occupied O 2p and Zn 3d/4sp states. All XES spectra show three similar distinct main features, but with different intensities. The three features at ~526, 523, and 520 eV were attributable mainly to O 2p-Zn 4sp and O 2p-Zn 3d hybridized states.^{7,8,11} The feature with the largest intensity is centered at ~526 eV and shift by ~0.15 eV upward in spectra a_1 and a_4 relative to those in spectra a_2 and a_3 , which indicate that oxygen atoms in ZnO nanorods are located at slightly nonequivalent sites.¹² The intensity of each feature decreases as the size of the *nc*-Au particles increases, suggesting that the number of electrons in the valence band of O 2p-derived states decreases as the size of the *nc*-Au particles increases. This trend implies that more electrons are transferred from the valence band to the conduction band of the *nc*-Au/ZnO nanorods. Consequently, the storage of electrons in larger *nc*-Au particles in S-3-10 exceeds those in S-4-10 and S-5-30 with smaller particles. This observation is consistent with the decrease in the intensities of the O *K*- and Zn, and Au *L*₃-edge XANES spectral features as the size of

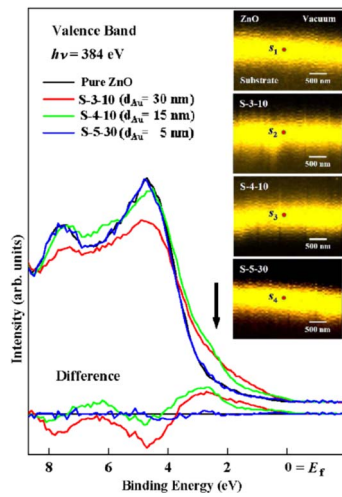


FIG. 4. (Color online) Valence-band photoemission spectra obtained from selected positions S_1 – S_4 shown in the upper inset, which presents the Zn 3d SPEM cross-sectional images of pure ZnO nanorods and *nc*-Au/ZnO nanorods. The lower inset shows the different valence-band spectra of *nc*-Au/ZnO nanorods and pure ZnO nanorods.

the *nc*-Au particles increases. Figure 3(b) presents XES and corresponding XANES spectra of O 2*p* states of *nc*-Au/ZnO nanorods and pure ZnO nanorods. A well-defined band gap between the valence-band maximum (VBM) and conduction-band minimum can be obtained for the various *nc*-Au/ZnO nanorods. This band gap, ~ 3.3 eV, is the same as that obtained by Dong *et al.* for nanostructured ZnO materials,⁷ suggesting that the band gap of *nc*-Au/ZnO nanorods is independent of the size of the *nc*-Au particles, although the *nc*-Au particles in this nanocomposited system acts crucially as a sink.

Figure 4 displays spatially resolved valence-band photoemission spectra of *nc*-Au/ZnO nanorods and pure ZnO nanorods. The Zn 3d SPEM images in the insets show cross-sectional views of nanorods, in which the bright areas have maximum Zn 3d intensities. The SPEM spectra show photoelectron yield from the selected areas in the sidewall regions of pure ZnO nanorods and *nc*-Au/ZnO nanorods indicated by S_1 – S_4 in the images. The energy of valence-band photoemission spectra has been calibrated by the E_f of a clean gold metal. The zero energy refers to VBM, which is the threshold of the emission spectrum and is also referred to as E_f . The two prominent features at ~ 4.5 and 7.5 eV in the spectra are dominated by the occupied O 2*p* states and the O 2*p* and Zn 4*sp* hybridized states of ZnO nanorods.¹³ The figure reveals that the intensities of the two main features decrease as the size of the *nc*-Au particles increases, so as the number of electrons in the valence band of O 2*p*-Zn 4*sp* hybridized states, consistent with the XES result presented in Fig. 3(a). In addition, a shoulder (indicated by an arrow) in the 0–4 eV region near/at E_f is present for larger *nc*-Au particles in the S-3-10 and S-4-10 samples. It is absent for the smaller *nc*-Au particles in the S-5-30 sample and pure ZnO nanorods. The electronic states close to E_f are generally known to be dominated by the transition metal *d* band in transition metal compounds.¹⁴ So, the density of states (DOS) near/at E_f can be attributed to Au 5*d* and O 2*p* hybridized states. The bottom of Fig. 4 shows the difference between the valence-band spectra of *nc*-Au/ZnO nanorods and pure ZnO nanorods, which is attributable to the Au 5*d* and Zn 4*sp* DOSs of the *nc*-Au/ZnO nanorods. The intensity

of the shoulder increases with the size of the *nc*-Au particles, as shown in the difference spectra of S-3-10 and S-4-10, providing evidence of the existence of Au 5*d* states near/at the E_f of the *nc*-Au/ZnO nanorods. The increase of the DOSs of Au 5*d* states with the *nc*-Au particle size agrees with Au L_3 -edge XANES and XRD results stated previously. Figure 4 demonstrates an important finding that the contact of *nc*-Au particles with ZnO nanorods promotes interfacial charge transfer and increases the DOSs of Au 5*d* states near/at the E_f , although the energy position of E_f in *nc*-Au/ZnO nanorods remains the same as that of pure ZnO nanorods.

In the previous study,⁴ the enhancement of the photocatalytic activity for the degradation of methyl orange under 365 nm irradiation is achieved by loading *nc*-Au particles with sizes smaller than 15 nm and is more pronounced as the size of the *nc*-Au particles is reduced to 5 nm, whereas the photocatalytic activity of *nc*-Au/ZnO nanorods is much lower than that of the ZnO nanorods when the size of the *nc*-Au particles is increased to 30 nm. In the present work, the XANES, XES, and SPEM results consistently show electron transfer from ZnO nanorods to *nc*-Au particles and the storage of electrons in *nc*-Au particles, which increase with the size of the *nc*-Au particles. It suggests that the enhancement of the photocatalytic activity of the ZnO nanorods is ascribed to the enrichment of the photoinduced charge separation by loading *nc*-Au particles. However, the dependence of charge separation ability on the size of the *nc*-Au particles demonstrated in this work is not fully consistent with the photocatalytic activity of the *nc*-Au/ZnO nanorods found by Wu and Tseng,⁴ suggesting that other factors such as scattering of the incident UV irradiation by the *nc*-Au particles may influence the photocatalytic activity of the *nc*-Au/ZnO nanorods as well.

This work was supported by the National Science Council of Taiwan under Contract No. NSC 95-2112-M032-014. The Advanced Light Source is supported by the U.S. Department of Energy under Contract No. DE-AC02-05CH11231.

¹A. Mills and S. L. Hunte, *J. Photochem. Photobiol.*, A **108**, 1 (1997).

²V. Subramanian, E. Wolf, and P. V. Kamat, *J. Am. Chem. Soc.* **126**, 4943 (2004).

³A. Wood, M. Giersig, and P. Mulvaney, *J. Phys. Chem. B* **105**, 8810 (2001).

⁴J. Wu and C. H. Tseng, *Appl. Catal.*, B **66**, 52 (2006).

⁵J. W. Chiou, J. C. Jan, H. M. Tsai, C. W. Bao, W. F. Pong, M.-H. Tsai, I.-H. Hong, R. Klausner, J. F. Lee, J. J. Wu, and S. C. Liu, *Appl. Phys. Lett.* **84**, 3462 (2004).

⁶J. W. Chiou, K. P. Krishna Kumar, J. C. Jan, H. M. Tsai, C. W. Bao, W. F. Pong, F. Z. Chien, M.-H. Tsai, I.-H. Hong, R. Klausner, J. F. Lee, J. J. Wu, and S. C. Liu, *Appl. Phys. Lett.* **85**, 3220 (2004).

⁷C. L. Dong, C. Persson, L. Vayssieres, A. Augustsson, T. Schmitt, M. Mattesini, R. Ahuja, C. L. Chang, and J.-H. Guo, *Phys. Rev. B* **70**, 195325 (2004).

⁸J.-H. Guo, L. Vayssieres, C. Persson, R. Ahuja, B. Johansson, and J. Nordgren, *J. Phys.: Condens. Matter* **14**, 6969 (2002).

⁹L. S. Hsu, Y.-K. Wang, Y.-L. Tai, and J. F. Lee, *Phys. Rev. B* **72**, 115115 (2005).

¹⁰P. Zhang and T. K. Sham, *Appl. Phys. Lett.* **81**, 736 (2002).

¹¹R. T. Girard, O. Tjernberg, G. Chiaia, S. Söderholm, U. O. Karlsson, C. Wigren, H. Nylén, and I. Lindau, *Surf. Sci.* **373**, 409 (1997).

¹²J.-H. Guo, S. M. Butorin, N. Wassdahl, P. Skytt, J. Nordgren, and Y. Ma, *Phys. Rev. B* **49**, 1376 (1994).

¹³J. W. Chiou, H. M. Tsai, C. W. Bao, K. P. Krishna Kumar, S. C. Ray, F. Z. Chien, W. F. Pong, M.-H. Tsai, C. H. Chen, H.-J. Lin, J. J. Wu, M. H. Yang, S. C. Liu, H. H. Chiang, and C. W. Chen, *Appl. Phys. Lett.* **89**, 043121 (2006).

¹⁴S. J. Naftel, A. Bzowski, and T. K. Sham, *J. Alloys Compd.* **283**, 5 (1999).